Since January 2020 Elsevier has created a COVID-19 resource centre with free information in English and Mandarin on the novel coronavirus COVID-19. The COVID-19 resource centre is hosted on Elsevier Connect, the company's public news and information website.

International Journal of Pharmaceutics 619 (2022) 121688

Contents lists available at ScienceDirect

International Journal of Pharmaceutics

journal homepage: www.elsevier.com/locate/ijpharm

Pharmacokinetics and safety of inhaled ivermectin in mice as a potential COVID-19 treatment

Ahmed H. Albariqi [a,b,1], Yuncheng Wang [a,1], Rachel Yoon Kyung Chang [a], Diana H. Quan [c], Xiaonan Wang [c], Stefanie Kalfas [d], John Drago [d,e], Warwick J. Britton [c,f], Hak-Kim Chan [a,*]

[a] Advanced Drug Delivery Group, Sydney Pharmacy School, Faculty of Medicine and Health, The University of Sydney, NSW 2006, Australia
[b] The Department of Pharmaceutics, Faculty of Pharmacy, Jazan University, Jazan 45142, Saudi Arabia
[c] Tuberculosis Research Program at the Centenary Institute, The University of Sydney, NSW 2006, Australia
[d] Florey Institute of Neuroscience and Mental Health, Melbourne, VIC 3052, Australia
[e] Department of Medicine, St Vincent's Hospital, University of Melbourne, VIC 3010, Australia
[f] Department of Clinical Immunology, Royal Prince Alfred Hospital, Camperdown, NSW 2050, Australia

ARTICLE INFO

Keywords:
COVID-19
Inhalable ivermectin
Lactose
Pharmacokinetics
Safety
Dry powder aerosol
Spray drying

ABSTRACT

Pharmacokinetic limitations associated with oral ivermectin may limit its success as a potential COVID-19 treatment based on *in vitro* experiments which demonstrate antiviral efficacy against SARS-CoV-2 at high concentrations. Targeted delivery to the lungs is a practical way to overcome these limitations and ensure the presence of a therapeutic concentration of the drug in a clinically critical site of viral pathology. In this study, the pharmacokinetics (PK) and safety of inhaled dry powders of ivermectin with lactose were investigated in healthy mice.

Female BALB/c mice received ivermectin formulation by intratracheal administration at high (3.15 mg/kg) or low doses (2.04 mg/kg). Plasma, bronchoalveolar lavage fluid (BALF), lung, kidney, liver, and spleen were collected at predetermined time points up to 48 h and analyzed for PK. Histological evaluation of lungs was used to examine the safety of the formulation.

Inhalation delivery of ivermectin formulation showed improved pharmacokinetic performance as it avoided protein binding encountered in systemic delivery and maintained a high exposure above the *in vitro* antiviral concentration in the respiratory tract for at least 24 h. The local toxicity was mild with less than 20% of the lung showing histological damage at 24 h, which resolved to 10% by 48 h.

1. Introduction

Despite two years of attempting to combat COVID-19, many countries are entering their most aggressive wave of daily cases to date (Johns Hopkins University, 2021). While many countries have achieved high vaccination coverage, vaccine access is variable across the world, and the emergence of the omicron variant has threatened to undermine the efficacy of the two-dose vaccine regime. (Callaway, 2021; Hadj Hassine, 2021; World Health Organization, 2021). Even before the emergence of the omicron variant, vaccine hesitancy, vaccine access inequity and vaccine responsiveness in various immunosuppressed vulnerable groups has contributed to ongoing morbidity and mortality from COVID-19 (Cornberg et al., 2021; Sallam, 2021; Wouters et al., 2021). Therefore, there is an urgent need to develop pharmacological treatments that can be given early in the disease course to reduce ultimate morbidity and mortality while also relieving the burden on the healthcare system and avoiding collateral damage from non-COVID-19 serious diseases.

Ivermectin is a broad spectrum antiparasitic agent that was first developed over 40 years ago. It has been shown to have antiviral properties *in vitro* against a range of viruses (Ōmura, 2008). It has been used successfully for over 30 years to treat various parasitic infections in humans and animals and has an established safety profile and wide safety margin (Gilbert and Slechta, 2018; Guzzo et al., 2002; Merck Sharp & Dohme BV, 2018; Nicolas et al., 2020; Ōmura and Crump, 2014). It is licensed for oral and topical use in humans, and oral, topical

* Corresponding author.
E-mail address: kim.chan@sydney.edu.au (H.-K. Chan).
[1] Ahmed H. Albariqi and Yuncheng Wang contributed equally to this work.

https://doi.org/10.1016/j.ijpharm.2022.121688
Received 2 February 2022; Received in revised form 14 March 2022; Accepted 15 March 2022
Available online 18 March 2022

and parenteral use in animals, with the standard dosing used typically between 150 and 400 μg/kg (Gilbert and Slechta, 2018). Ivermectin has been shown to clear coronavirus in transfected Vero-hSLAM cells *in vitro* at concentrations of approximately 5 μM, presumably by preventing nuclear import of the viral RNA through the importin α/β receptor. This concentration is equivalent to 4,370 ng/mL, approximately 50–100-fold greater than the peak concentration (C_{max}) achieved after a single oral dose of 200 μg/kg (Chaccour et al., 2017). Even very high oral doses of ivermectin dosed at 2,000 μg/kg, while demonstrated to be safe, produce C_{max} values that are 10–20 times lower than required to attain plasma concentrations of 5 μM (Guzzo et al., 2002).

Thus, the concern with ivermectin as a therapy for COVID-19 is that it will be difficult to achieve the concentrations of ivermectin demonstrated to be necessary to inhibit viral replication *in vitro* using oral therapy in human subjects without dose limiting side effects (Lundberg et al., 2013). Despite pharmacokinetic studies in cattle and goats demonstrating a high distribution of ivermectin to the lungs following subcutaneous administration, the highest C_{max} level achieved with a subcutaneous dose of 200 μg was >40 times less than the 5 μM antiviral concentration required to achieve an antiviral effect *in vitro* (Lv et al., 2018; Mastrangelo et al., 2012). Furthermore, due to the strong plasma protein binding of ivermectin, even high doses when administered orally may not be sufficient to reach the half maximal inhibitory concentration (IC_{50}) required for ivermectin activity against SARS-CoV-2 (Gatti and De Ponti, 2021).

These pharmacological considerations highlight the need for a mode of ivermectin delivery that is specifically targeted to the lungs and respiratory tract, particularly as this is the predominant site of viral entry. Targeted delivery of ivermectin to the lungs may achieve the effective local concentration with much lower total doses, while bypassing plasma protein binding and avoiding systemic toxicity.

Several animal experiments have reported that direct pulmonary delivery of ivermectin can be achieved safely. Importantly, safety has also been demonstrated at doses that align with antiviral concentrations (Chaccour et al., 2020). The safety of intranasal and nebulized ivermectin has also been examined more recently in pigs and rats, with results corroborating the safety of direct respiratory delivery. Intranasal ivermectin was well tolerated in pigs at a dose of 0.2 mg/kg, although repeated daily dosing that would be required to achieve antiviral concentrations was not tested (Errecalde et al., 2021). Lung toxicity was observed in rats only with high doses of inhaled ivermectin at ≥0.2 mg/kg, while lower doses of 0.05 to 0.1 mg/kg were not associated with demonstrable toxicity (Mansour et al., 2021). This is in contrast to a study of nebulized ivermectin in an alcoholic solution in rats which reported safety in doses of 140 mg/kg. Interpretation of this study is complicated by the fact that the pharmacokinetic data of nebulized ivermectin did not fully represent the inhaled delivery paradigm because most of the drug was swallowed (Chaccour et al., 2020).

Recently, we have prepared and characterized spray-dried, inhalable dry powders of ivermectin with lactose crystals as an excipient for potential treatment of COVID-19 (Albariqi et al., 2022). The ratio of the drug to excipient was optimized to deliver an anticipated dose of 125 μg for humans based on the reported concentration for viral inactivation of 5 μM and the volume of lung lining fluid being 25 mL (Caly et al., 2020; Dinesh Kumar et al., 2021; Walters, 2002). The powder formulation showed stable solid-state properties and excellent *in vitro* aerosol performance with fine particle dose of ≈ 300 μg when dispersed by a medium-high resistance Osmohaler at a flow rate of 60 L/min.

In this study, we have investigated the pharmacokinetics (PK) and evaluated the local toxicity of the inhalable dry powders of ivermectin and lactose crystals in healthy mice. The dry powder formulation was delivered by intratracheal insufflation. The PK were assessed in the plasma, bronchoalveolar lavage fluid (BALF), lung, liver, kidney, and spleen. The local toxicity was examined in the lung tissue by histological analysis.

2. Materials and methods

2.1. Materials

Ivermectin was obtained from Hovione PharmaScience Ltd (Tapa, Macau). Alpha-lactose monohydrate (LH300) was sourced from DFE Pharma (Goch, Germany), isopropanol from Sigma-Aldrich Pty. Ltd (Sydney, Australia), methanol and acetonitrile from Merck KGaA (Darmstadt, Germany). The water utilized in this study was purified by an SG ultra-pure system (Barsbüttel, Germany).

2.2. Powder preparation

Ivermectin was dissolved in isopropanol followed by suspending the lactose crystals at concentrations of 2.4 and 45.6 mg/mL, respectively, to obtain a weight ratio of ivermectin to lactose of 1:19. These concentrations and ratio were chosen based on our previous study which optimized the inhalable dose for human airways in order to achieve the reported *in vitro* antiviral concentration of 5 μM (Albariqi et al., 2022). Dry powders were prepared by spray drying (B-290 spray dryer connected to B-295 inert loop, Buchi Laboratories, Flawil, Switzerland) conducted in the closed loop mode, with the conditions set at inlet temperature of 70 °C, atomization nitrogen rate of 601 L/hr, aspiration of 38.2 m^3/hr, and feed intake of 15 mL/min.

2.3. Animal procedures

Eight- to ten-week-old female BALB/c mice (20.0 ± 0.94 g) were obtained from Animal Recourses Center (Perth, Australia) and kept in the animal facility of the Centenary Institute of Cancer Medicine and Cell Biology (Camperdown, Australia). The animal procedures were conducted with approval of Sydney Local Health District (SLHD) Animal Welfare Committee (Protocol number: 2019/017).

2.4. Intratracheal delivery

The intratracheal delivery was conducted using a dry powder loading device made of a 200 μL gel loading pipette tip attached to a 1 mL syringe through a three-way stopcock valve (Qiu et al., 2020). A known amount of the powder formulation was filled in pre-weighed tips prior the experiments, taking into consideration the maximal and minimal loading capacity of the tips being 1 and 2 mg, respectively. The animal was anesthetized by intraperitoneal injection of ketamine/ xylazine (100/10 mg/kg) and placed on an intubation stand. The loading tip was inserted into the trachea with help of an otoscope (MDS, Hallowell EMC, Pittsfield, MA, United states) and a guiding cannula. The powder was dispersed with a volume of 0.4 mL air by the syringe. The delivered dose was determined by the weight difference in the tips before and after the dispersion.

2.5. Dose selection

The pharmacokinetics of ivermectin were examined using two doses: lower and higher doses. The lower dose was selected based on mathematical scaling of systemic human dose to animal dose with the following equation (Phillips, 2017):

$$Xh = Xa\left(\frac{Ma}{Mh}\right)^{(1-b)}$$

where Xh is human dose normalized to body mass, Xa animal dose normalized to body mass, Ma animal body mass, Mh human body mass, and b the allometric exponent constant of 0.67. The loading tips were filled to achieve a lower dose of 2.10 mg/kg according to the equation. In practice, the actual dose delivered to the lungs of the mice was 2.04 ± 0.40 mg/kg. The higher dose was selected based on maximal loading

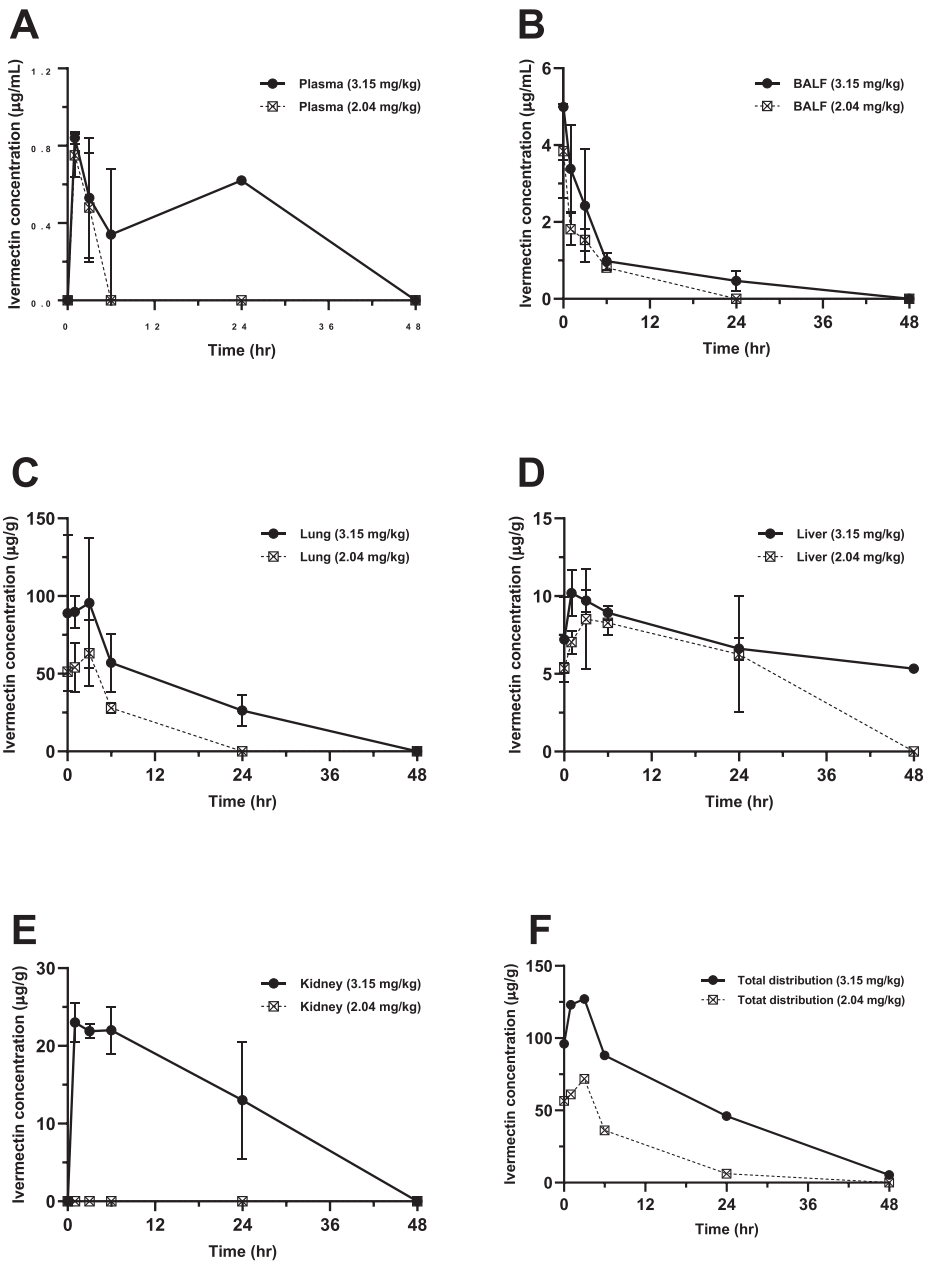

Fig. 1. Ivermectin concentrations over time following intratracheal (IT) delivery of the two doses to BALB/c mice ($n = 4$) for: (A) plasma, (B) bronchoalveolar lavage (BALF) fluid, (C) lung, (D) liver, (E) kidney and (F) the sum distribution of ivermectin in lung, liver, and kidney. The data are shown as the means +/− SD.

capacity of the tips of the delivery device. The delivered dose to the lungs was 3.15 ± 0.60 mg/kg.

For the histological study, only the lower dose was examined as it is the equivalent to the systemic human dose.

2.6. Sample collection and processing for PK

Six groups of four mice were used for each dose. The mice were euthanized by carbon dioxide at the allocated time points (0, 1, 3, 6, 24, 48 h after dose delivery). Blood, BALF, lungs, liver, kidneys, and spleen were collected and processed for HPLC assay. Blood was collected in ethylenediaminetetraacetic acid (EDTA) tubes, centrifuged to separate plasma using a Beckman Coulter Allegra X-12R Centrifuge (Pasadena, CA, United States) at a temperature of 4 °C and 2500 rpm for 10 min. The plasma was deproteinated with acetonitrile at a ratio of 1:3 (v/v) and recentrifuged, then the supernatant was collected. The lungs were washed three times with 1 mL of phosphate buffered saline to collect bronchoalveolar lavage fluid (BALF). This was then deprotonated with an equivalent amount of acetonitrile, centrifuged to remove cellular debris, and the supernatant collected. Lungs, liver, kidneys and spleen were harvested in 2 mL of triply deionised water, homogenized with a Polytron PT10-35 homogenizer connected to PCU power control unit (Kinematica AG Littau/Luzern, Switzerland), and processed as for plasma. All processed samples were kept in ice until chemical assay of ivermectin was performed.

2.7. Chemical analysis of ivermectin in the samples

Shimadzu high performance liquid chromatography (HPLC, Kyoto, Japan) with a Phenomenex Luna C18(2) 100 Å 5 µm 4.6 × 250 mm column was used to quantify the concentration of ivermectin in the samples after being filtered with 0.45 µm polytetrafluoroethylene

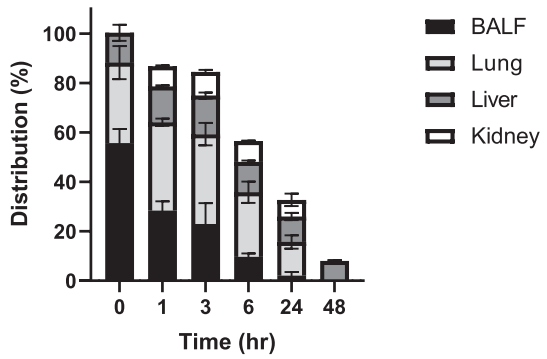

Fig. 2. Distribution of ivermectin in BALF, lung, liver, and kidney over time following intratracheal delivery of the two doses. Data are the mean % distribution +/− SD (n = 8 mice).

Table 1
Pharmacokinetic parameters of inhaled ivermectin following intratracheal administration in BALB/c mice.

Dose		*Ke*	$t_{1/2}$	T_{max}	C_{max}	$AUC_{0-\infty}$	CL	V_d
mg/kg		1/hr	Hr	hr	μg/mL or μg/g	μg.hr/mL or μg.hr/g	mL/kg.hr or g/kg.hr	mL/kg or g/kg
3.15	Plasma	*ND*	*ND*	1	0.84	*ND*	*ND*	*ND*
	BALF	0.09	7.90	0	4.99	33.55	0.094	1.07
	Lung	0.05	12.6	3	96.6	1734	0.002	0.03
	Liver	0.01	50.3	1	10.2	726.8	0.004	0.31
	Kidney	0.03	27.4	1	23.0	935.4	0.003	0.13
2.04	Plasma	*ND*	*ND*	1	0.75	*ND*	*ND*	*ND*
	BALF	0.16	4.23	0	3.84	14.64	0.139	0.85
	Lung	ND	ND	3	63.2	ND	ND	ND
	Liver	0.02	46.0	3	8.52	591.9	0.003	0.23
	Kidney	*NA*	*NA*	*NA*	*NA*	*NA*	*NA*	*NA*

ND: not determined
NA: not applicable

(PTFE) membrane to protect the column from any tissue residuals. The mobile phase consisted of water, methanol, and acetonitrile (15:34:51 v/v), running at a flow rate of 1 mL/min. The injection volume was set at 100 μL for the plasma samples and 20 μL for the other samples. The UV detection wavelength was 254 nm, and the lower limit of quantification was 140 ng/mL.

2.8. Pharmacokinetic analysis

Non-compartmental model was applied to determine the PK profile of inhaled ivermectin. Maximum concentration (C_{max}) and time to maximum concentration (T_{max}) were determined directly form the plots, while other parameters, including the elimination rate constant (*Ke*), half-life time ($t_{1/2}$), total drug exposure ($AUC_{0-\infty}$), clearance (CL) and volume of distribution (V_d), were determined using PKSolver, an add-in tool available for Microsoft excel (Zhang et al., 2010).

2.9. Histological analysis

The local toxicity of inhaled ivermectin was evaluated with the single dose of 2.04 ± 0.40 mg/kg over different time points. Groups of three mice were used for treatment (0, 24, and 48 h after dose delivery), and control (no treatment, air only, lactose only for 24 and 48 h). The mice were euthanized with carbon dioxide at predetermined time points. Lungs were perfused with 10 mL of phosphate buffered saline through the pulmonary artery, harvested, and fixed in 10% neutral buffered formalin. The histological examination was conducted in Phenomics Australia Histopathology and Slide Scanning Service at the University of Melbourne (Parkville, VIC, Australia) to demonstrate the collective extent of damage in a grading scale (0 for no or mild change, 1 for damage of less than 25%, 2 for damage between 25 and 50%, and 3 for damage greater than 50%).

3. Results

3.1. Ivermectin PK analysis

The concentration of ivermectin in plasma, BALF, and other tissues over time; the distribution in BALF and other tissues over time; and pharmacokinetic parameters with two doses following intratracheal administration are presented in Figs. 1, 2 and Table 1 respectively. Ivermectin was detected in the plasma, BALF, lung, and liver with both doses, but was only detected in the kidney at the higher dose. Except for C_{max} and T_{max}, the PK parameters were not determined for plasma at both doses and for the lung tissue at the lower dose because less than three points in terminal elimination phase could be detected. No data are shown for the spleen as the drug was not detected there.

For both the higher and lower doses, the plasma drug concentration increased to a peak (C_{max}: 0.84 ± 0.03 and 0.75 ± 0.11 μg/mL, respectively) in 1 h, followed by a steep decline until complete elimination at 6 h after the lower dose and at 24 h following the higher dose (Fig. 1-A).

The maximum ivermectin concentration in the BALF for both the higher and lower doses were detected immediately at time 0 (4.99 ± 1.38 and 3.84 ± 1.23 μg/mL, respectively), and continued to decline until no drug was identified at 48 and 24 h, respectively (Fig. 1-B). This was associated with a $t_{1/2}$ of 7.90 and 4.24 h, respectively, and a total drug exposure ($AUC_{0-\infty}$) of 33.55 and 14.64 μg.hr/mL, respectively.

The distribution of ivermectin in the lung tissue took 3 h to reach the T_{max} with a C_{max} of 95.6 ± 41.9 and 63.2 ± 21.4 μg/g, respectively, for the higher and lower doses (Fig. 1-C). After the higher dose, ivermectin was detectable in lung tissue for 48 h, while there was no drug detected at 24 h with the lower dose. The $AUC_{0-\infty}$ and $t_{1/2}$ of the higher dose were 1734 μg.hr/g and 12.6 h, respectively.

Analysis of the liver tissue showed a C_{max} of 10.21 ± 1.49 and 8.52 ± 3.22 μg/g with different T_{max} values of 1 and 3 h for the higher dose and lower doses, respectively (Fig. 1-D). At 48 h after the higher dose, the ivermectin concentration had reduced by half (5.33 ± 0.27 μg/g), while no drug was detectable with the lower dose. Thus, the total liver drug exposure values were 726.8 and 591.9 μg.hr/g with $t_{1/2}$ of 50.3 and 46 h, respectively, for the higher and lower doses. The kidney drug concentration for the higher dose was peaked (C_{max}: 23 μg/g) at 1 h with an $AUC_{0-\infty}$ and $t_{1/2}$ of 935.4 μg.hr/g and 27.4 h, respectively (Fig. 1-E).

A clear dose-dependent pattern was shown in Fig. 1-F with a peak at 3 h and availability up to 48 h when the tissue concentrations of ivermectin in lung, liver, and kidney were added together for each dose in order to estimate the relationship between the dose and tissue distribution over time after intratracheal delivery.

Fig. 2 shows the distribution of ivermectin in BALF and other tissues over time relative to the initial dose. At time 0 immediately after dosing, ivermectin was primarily in the respiratory tract. At 24 h, the lung tissue retained only 13.6 ± 4.71% of ivermectin while liver and kidney showed 10.3 ± 2.47% and 6.71 ± 4.35%, respectively. At 48 h, ivermectin distributed exclusively in the liver tissue showing 8 ± 0.63% of the initial dose.

3.2. Histological analysis

The histological appearance of lungs after intratracheal administration of ivermectin at the single dose of 2.04 ± 0.40 mg/kg are presented in Fig. 3 and summarized Table 2. In general, control mice which did not

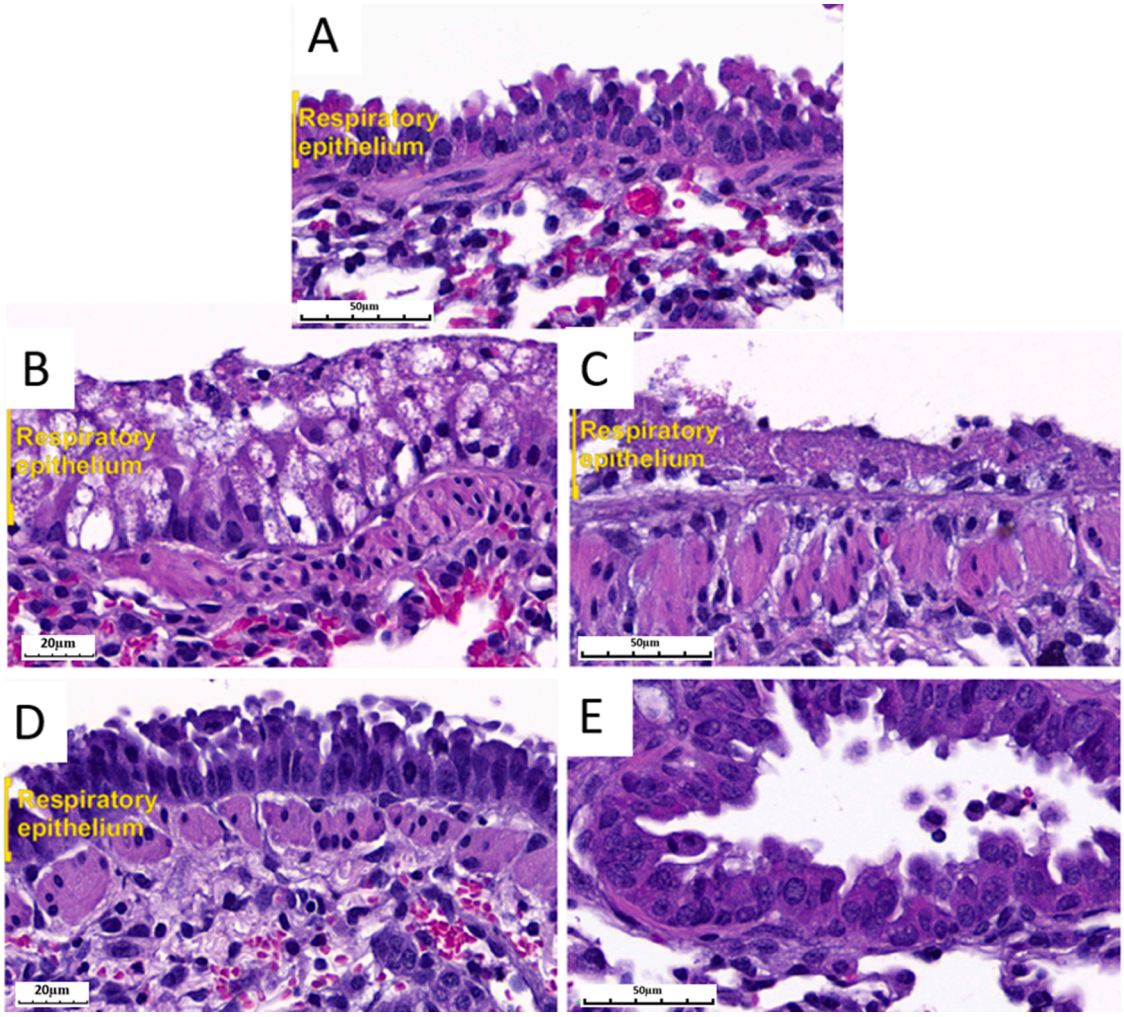

Fig. 3. Representative images of the lung histology in BALB/c mice that received ivermectin at dose of 2.04 ± 0.40 mg/kg or lactose only at magnification of 40X (B, and D) or 20X (A, C, E). Untreated mice showed normal epithelium (A). Necrotic and vacuolated epithelium areas were evident with ivermectin (B) and lactose only (C) at 24 h after delivery. Regenerated respiratory epithelium was evident with ivermectin (D) and lactose only (E) at 48 h after delivery. (Hematoxylin and Eosin staining).

Table 2
Histological evaluation of the lungs of BALB/c mice following intratracheal administration in spray-dried ivermectin.

Group	Grade	Comment
No treatment	0	
Air only	0	
Lactose only (24 h)	1	Lung area 15%
Lactose only (48 h)	1	Lung area 1–5%
Treatment (Time 0)	0	
Treatment (24 h)	1	Lung area 20%
Treatment (48 h)	1	Lung area 2–10%

Grade 0 = no changes/mild changes considered insignificant
Grade 1 = minimal lesions affecting 1–25% of the area
Grade 2 = multifocal lesions affecting 25–50% of the area
Grade 3 = severe tissue changes affecting >50% of the area

receive powder insufflation (no treatment, air only) showed intact tissues, and were scored at 0 (Fig. 3-A). Control groups that received intratracheal lactose powder (Fig. 3-C and E), showed minimal lesions affecting 15% of the lung at 24 h and this resolved to 1–5% at 48 h. These were scored at 1.

The local changes observed in the treatment groups varied in extent and grade over time. The respiratory epithelium was intact at time 0. Transient lung inflammation affecting 20% of the lung with markedly vacuolated epithelium was observed at 24 h after ivermectin delivery (Fig. 3-B). However, these lung changes had resolved to affect 2–10% of the lung with regenerated intact epithelium at 48 h (Fig. 3-D). Since the multifocal lesions affected <25% of lung area, the collective damage of both treatment groups at 24 and 48 h were scored at 1.

4. Discussion

In this study, the effect of delivery to the lungs of inhalable dry powders of ivermectin coated on lactose crystals were examined pharmacokinetically and histologically in a BALB/c mouse model. The *in vitro* antiviral activity of ivermectin against SARS-CoV-2 has been reported in previous studies have an IC_{50} of 2.5 μM (Caly et al., 2020; Dinesh Kumar et al., 2021).

The inhalable powder of ivermectin and lactose was formulated to deliver 125 μg for human to achieve the antiviral concentration of 5 μM. The PK study was conducted for two doses. The lower dose (2.04 ± 0.40 mg/kg) was mathematically scaled from the systemic human dose, while the higher dose (3.15 ± 0.60 mg/kg) was based on the maximal loading capacity of the intratracheal delivery device. Ivermectin was successfully delivered to the pulmonary tract and maintained concentrations remarkably above the *in vitro* antiviral concentration in the lung tissue

and BALF for at least 24 h after administration. Doses of 2.04 ± 0.40 mg/kg of inhaled ivermectin were deemed to be well tolerated and achieved a C_{max} greater than 10 times the *in vitro* antiviral concentration. The lipophilic nature of ivermectin and its large volume of distribution may explain the high drug exposure in lung tissue noted in other non-rodent animal pharmacokinetic studies (Lespine et al., 2005; Lifschitz et al., 2000). In addition, our results are consistent with a study showing that the local delivery of ivermectin *via* the nasal route achieved significantly higher nasopharynx and lungs/plasma ratios compared to oral delivery (Errecalde et al., 2021). The validation of high ivermectin drug exposure in the lung tissue compared to plasma and other tissues when delivered through inhalation is critical from an antiviral therapeutic perspective.

Because of the protein binding affinity and hydrophobicity of ivermectin, it was expected that lower levels of plasma ivermectin would be observed after intratracheal insufflation. However, since the detected levels of ivermectin in the plasma were not sufficient to provide a complete pharmacokinetic profile, it is not possible to make a direct comparison with other published data of systemic delivery of ivermectin. Generally, ivermectin is absorbed into the systemic circulation from the gastrointestinal tract, metabolized in the liver and excreted in the faeces with less than 1% of the drug undergoing renal excretion, showing a half-life of 80 h (Gonzalez Canga et al., 2008; Guzzo et al., 2002). The inhaled ivermectin dry powder formulation was absorbed from the lung tissue into the systemic circulation and then distributed to other organs. Therefore, ivermectin was detected in the plasma, BALF, lung, and liver with both doses, but was only detected in the kidney at the higher dose and only up to 24 h. The PK of ivermectin in the liver and kidney tissues were consistent with these published data, showing the trend for hepatic elimination (up to 48 h) with a half-life of 50 h, and lower renal distribution of less than 7% at 24 h. In addition, the low plasma concentration of ivermectin with the low dose beside the low renal clearance may explain the difference between the high dose and low dose of ivermectin in the kidneys.

The safety of inhaled ivermectin was assessed after intratracheal instillation of ivermectin as liquid to rats using different doses in a recent study (Mansour et al., 2021). The histological evaluation was conducted after repeating doses for three days. The local toxicity in the lung was found to be dose-dependent, and doses below 0.1 mg/kg were considered to be safe. Our histological findings revealed that inhaled ivermectin can be considered safe in mice with dose equivalent to oral human dose as there was no difference between lung change caused by the ivermectin-containing formulation or the lactose-only control, and lactose is an approved excipient for pulmonary drugs in humans (Pilcer and Amighi, 2010). Moreover, we demonstrate that delivery of our dry powder formulations are able to achieve the *in vitro* antiviral concentrations of ivermectin in the BALF and lung tissue.

5. Conclusion

Inhaled delivery of this dry powder ivermectin formulation achieved high concentrations of the drug in the lung and BALF tissue, exceeding concentrations required for antiviral efficacy based on *in vitro* studies.

Funding

No funding was received for this study.

CRediT authorship contribution statement

Ahmed H. Albariqi: Conceptualization, Methodology, Investigation, Formal analysis, Data curation, Visualization, Writing – original draft. **Yuncheng Wang:** Validation, Methodology, Investigation, Formal analysis, Data curation. **Rachel Yoon Kyung Chang:** Conceptualization, Validation, Data curation. **Diana H. Quan:** Methodology, Investigation. **Xiaonan Wang:** Methodology, Investigation. **Stefanie Kalfas:** Formal analysis, Data curation, Writing – review & editing. **John Drago:** Formal analysis, Data curation, Writing – review & editing. **Warwick J. Britton:** Conceptualization, Resources, Supervision, Writing – review & editing. **Hak-Kim Chan:** Conceptualization, Resources, Supervision, Writing – review & editing.

Declaration of Competing Interest

The authors declare the following financial interests/personal relationships which may be considered as potential competing interests: JD, HKC, and AHA are inventors of a provisional patent (Australian application number: 2021902130) on inhaled ivermectin filed by the University of Sydney.

Acknowledgements

Ahmed H. Albariqi is sponsored by Jazan University (Saudi Arabia). H-K C is indebted to The Jack & Robert Smorgon Families Foundation for their generous financial support as a gift to the University of Sydney.

References

Albariqi, A.H., Ke, W.R., Khanal, D., Kalfas, S., Tang, P., Britton, W.J., Drago, J., Chan, H. K., 2022. Preparation and Characterisation of inhalable ivermectin powders as a potential COVID-19 therapy. J. Aerosol Med. Pulm. Drug Deliv. 35, 1–13.

Callaway, E., 2021. Omicron likely to weaken COVID vaccine protection. Nature 600 (7889), 367–368.

Caly, L., Druce, J.D., Catton, M.G., Jans, D.A., Wagstaff, K.M., 2020. The FDA-approved drug ivermectin inhibits the replication of SARS-CoV-2 in vitro. Antiviral Res. 178, 104787.

Chaccour, C., Abizanda, G., Irigoyen-Barrio, A., Casellas, A., Aldaz, A., Martinez-Galan, F., Hammann, F., Gil, A.G., 2020. Nebulized ivermectin for COVID-19 and other respiratory diseases, a proof of concept, dose-ranging study in rats. Sci. Rep. 10, 17073.

Chaccour, C., Hammann, F., Rabinovich, N.R., 2017. Ivermectin to reduce malaria transmission I. Pharmacokinetic and pharmacodynamic considerations regarding efficacy and safety. Malar. J. 16, 161.

Cornberg, M., Buti, M., Eberhardt, C.S., Grossi, P.A., Shouval, D., 2021. EASL position paper on the use of COVID-19 vaccines in patients with chronic liver diseases, hepatobiliary cancer and liver transplant recipients. J. Hepatol. 74 (4), 944–951.

Dinesh Kumar, N., Ter Ellen, B.M., Bouma, E.M., Troost, B., van de Pol, D.P.I., van der Ende-Metselaar, H.H., van Gosliga, D., Apperloo, L., Carpaij, O.A., van den Berge, M., Nawijn, M.C., Stienstra, Y., Rodenhuis-Zybert, I.A., Smit, J.M., 2021. Moxidectin and Ivermectin Inhibit Sars-Cov-2 Replication in Vero E6 Cells but Not in Human Primary Airway Epithelium Cells. Antimicrob. Agents Chemother., AAC0154321.

Errecalde, J., Lifschitz, A., Vecchioli, G., Ceballos, L., Errecalde, F., Ballent, M., Marín, G., Daniele, M., Turic, E., Spitzer, E., Toneguzzo, F., Gold, S., Krolewiecki, A., Alvarez, L., Lanusse, C., 2021. Safety and Pharmacokinetic Assessments of a Novel Ivermectin Nasal Spray Formulation in a Pig Model. J. Pharm. Sci. 110 (6), 2501–2507.

Gatti, M., De Ponti, F., 2021. Drug Repurposing in the COVID-19 Era: Insights from Case Studies Showing Pharmaceutical Peculiarities. Pharmaceutics 13 (3), 302.

Gilbert, B.W., Slechta, J., 2018. A Case of Ivermectin-Induced Warfarin Toxicity: First Published Report. Hosp. Pharm. 53 (6), 393–394.

Gonzalez Canga, A., Sahagun Prieto, A.M., Diez Liebana, M.J., Fernandez Martinez, N., Sierra Vega, M., Garcia Vieitez, J.J., 2008. The pharmacokinetics and interactions of ivermectin in humans – a mini-review. AAPS J. 10, 42–46.

Guzzo, C.A., Furtek, C.I., Porras, A.G., Chen, C., Tipping, R., Clineschmidt, C.M., Sciberras, D.G., Hsieh, J.Y., Lasseter, K.C., 2002. Safety, tolerability, and pharmacokinetics of escalating high doses of ivermectin in healthy adult subjects. J. Clin. Pharmacol. 42, 1122–1133.

Hadj Hassine, I., 2021. Covid-19 vaccines and variants of concern: A review. Rev, Med. Virol., p. e2313

Johns Hopkins University, 2021. COVID-19 Map - Johns Hopkins Coronavirus Resource Center.

Lespine, A., Alvinerie, M., Sutra, J.-F., Pors, I., Chartier, C., 2005. Influence of the route of administration on efficacy and tissue distribution of ivermectin in goat. Vet. Parasitol. 128 (3-4), 251–260.

Lifschitz, A., Virkel, G., Sallovitz, J., Sutra, J.F., Galtier, P., Alvinerie, M., Lanusse, C., 2000. Comparative distribution of ivermectin and doramectin to parasite location tissues in cattle. Vet. Parasitol. 87 (4), 327–338.

Lundberg, L., Pinkham, C., Baer, A., Amaya, M., Narayanan, A., Wagstaff, K.M., Jans, D. A., Kehn-Hall, K., 2013. Nuclear import and export inhibitors alter capsid protein distribution in mammalian cells and reduce Venezuelan Equine Encephalitis Virus replication. Antiviral Res. 100 (3), 662–672.

Lv, C., Liu, W., Wang, B., Dang, R., Qiu, L., Ren, J., Yan, C., Yang, Z., Wang, X., 2018. Ivermectin inhibits DNA polymerase UL42 of pseudorabies virus entrance into the nucleus and proliferation of the virus in vitro and vivo. Antiviral Res. 159, 55–62.

Mansour, M., Shamma, N., Ahmed, A., Sabry, A., Esmat, G., Mahmoud, A., Maged, 2021. Safety of inhaled ivermectin as a repurposed direct drug for treatment of COVID-19: A preclinical tolerance study. Int. Immunopharmacol. 99, 108004.

Mastrangelo, E., Pezzullo, M., De Burghgraeve, T., Kaptein, S., Pastorino, B., Dallmeier, K., de Lamballerie, X., Neyts, J., Hanson, A.M., Frick, D.N., Bolognesi, M., Milani, M., 2012. Ivermectin is a potent inhibitor of flavivirus replication specifically targeting NS3 helicase activity: new prospects for an old drug. J. Antimicrob. Chemother. 67 (8), 1884–1894.

Merck Sharp & Dohme BV Stromectol (Ivermectin): Product Information. Merck 2018 Sharp & Dohme Corp., Netherlands.

Nicolas, P., Maia, M.F., Bassat, Q., Kobylinski, K.C., Monteiro, W., Rabinovich, N.R., Menéndez, C., Bardají, A., Chaccour, C., 2020. Safety of oral ivermectin during pregnancy: a systematic review and meta-analysis. Lancet Glob Health 8 (1), e92–e100.

Ōmura, S., 2008. Ivermectin: 25 years and still going strong. Int. J. Antimicrob Agents 31 (2), 91–98.

Ōmura, S., Crump, A., 2014. Ivermectin: panacea for resource-poor communities? Trends Parasitol 30 (9), 445–455.

Phillips, J.E., 2017. Inhaled efficacious dose translation from rodent to human: A retrospective analysis of clinical standards for respiratory diseases. Pharmacol. Ther. 178, 141–147.

Pilcer, G., Amighi, K., 2010. Formulation strategy and use of excipients in pulmonary drug delivery. Int. J. Pharm. 392 (1-2), 1–19.

Qiu, Y., Liao, Q., Chow, M.Y.T., Lam, J.K.W., 2020. Intratracheal Administration of Dry Powder Formulation in Mice. J Vis Exp.

Sallam, M., 2021. COVID-19 Vaccine Hesitancy Worldwide: A Concise Systematic Review of Vaccine Acceptance Rates 2021 Vaccines (Basel) 9.

Walters, D.V., 2002. Lung lining liquid - the hidden depths. The 5th Nils W. Svenningsen memorial lecture. Biol. Neonate 81 (Suppl. 1), 2–5.

World Health Organization, 2021. Tracking SARS-CoV-2 variants.

Wouters, O.J., Shadlen, K.C., Salcher-Konrad, M., Pollard, A.J., Larson, H.J., Teerawattananon, Y., Jit, M., 2021. Challenges in ensuring global access to COVID-19 vaccines: production, affordability, allocation, and deployment. Lancet 397 (10278), 1023–1034.

Zhang, Y., Huo, M., Zhou, J., Xie, S., 2010. PKSolver: An add-in program for pharmacokinetic and pharmacodynamic data analysis in Microsoft Excel. Comput. Methods Programs Biomed. 99 (3), 306–314.